

Article

Relationship between Peak Stage, Storm Duration, and Bank Storage along a Meandering Stream

Lucas P. Chabela and Eric W. Peterson * 

Department of Geography, Geology, and the Environment, Illinois State University, Campus Box 4400, Normal, IL 61704, USA

* Correspondence: ewpeter@ilstu.edu; Tel.: +1-309-438-7865; Fax: +1-309-438-5310

Received: 11 July 2019; Accepted: 12 August 2019; Published: 15 August 2019



Abstract: Groundwater and surface water are often studied as different systems; however, one commonly affects the other. Bank storage, the temporary storage and release of stream water in adjacent aquifers, can contribute a considerable amount of discharge to a river and can be a component in the transport and fate of a contaminant. Studies document the effects of increasing stage and increasing storm duration; however, these controls are often investigated separately. This project examined which factor, peak stage or storm duration, was more influential on the bank-storage process. The study focused on a small reach of a third-order, meandering, perennial stream. A 3-D, transient-state numerical model (MODFLOW) was created of the study site, and 36 simulations were run at various peak stages and storm durations. Peak stage and storm durations, while both influential, affected different areas of the bank-storage process. Peak stage was statistically more influential in controlling the maximum volume of bank storage (~3.6×) and the volume of the storage that remained in the system at 100 h (~1.1×). Longer storm duration generated a slower return of water, thus increasing the retention of bank storage. Parafluvial exchange was an important factor in bank storage along a meandering stream, suggesting that at least 2-D, ideally 3-D, models need to be employed in evaluating bank storage.

Keywords: bank storage; groundwater modeling; MODFLOW; meandering streams

1. Introduction

Along any stream, interaction between the stream and the surrounding groundwater occurs. Basic interactions include streams gain water from the groundwater (gaining streams), streams lose water to the groundwater (losing streams), and streams gain and lose simultaneously along the entire stream [1]. Another type of interaction is parafluvial exchange across a meander bend, which is due to the increase in hydraulic gradient across the bend [2–4]. Parafluvial exchange can be an important source of interaction where meanders are the dominant river pattern [2]. Exchange processes from groundwater and surface water are controlled by the distribution and magnitude of hydraulic conductivities within the channel and surrounding sediments, the relation of stream stage to groundwater level, and the geometry and position of the stream channel within an alluvial flood plain [5–7]. Since water interacts horizontally and vertically, flow dynamics and direction are typically three-dimensional [7,8]. Understanding of the basic principles of interactions between groundwater and surface water is needed for effective management of water resources because contamination of one system can commonly affect the other [1,7].

An interaction that occurs in nearly all rivers is the infiltration of water into the stream banks due to an increase in stream stage [1]. An increase in stage can occur from storm precipitation, rapid snowmelt, or the release of water from an upstream reservoir. Precipitation events alter hydraulic head, which controls the direction of flow [9]. In a gaining stream, an increase in stream stage temporarily

reverses the normal groundwater hydraulic gradient away from the stream [10]. Water from the stream then infiltrates into the stream bank and the streambed, which displaces pre-existing groundwater or hyporheic water and recharges the adjacent aquifer [4,9,10]. As the stage falls and the hydraulic gradient returns to pre-storm stage, some or all of the infiltrated water returns to the river [1,10]. The process where water is temporarily stored in the stream banks and later returned is called bank storage. Complete saturation is generally not achieved due to the short duration of the elevated flow [11].

Bank storage has important hydrological and ecological implications, directly affecting the sediments surrounding the stream [12]. Studies document that bank-stored water can contribute a considerable volume of discharge to the river [11,13]. With this, return discharge of the bank-stored water can contaminate the surface water [10]. High concentrations of atrazine have been observed returning from the bank sediments with the return into the river during baseflow conditions [14].

Bank storage, like many hydrologic processes, can vary spatially and temporally due to the many controls. Hydrologic controls include: sinuosity of the stream [2,3,15,16], stream stage (discharge) [17–19], storm duration, period of length at which a peak stage is maintained [17,18], transmissivity of an aquifer [9,18], storage capacity of an aquifer [9], the presence or absence of an unsaturated zone [20], bank slope [14,18,20], and heterogeneity/homogeneity of an aquifer [15].

The volume of bank storage depends on the duration, height, and shape of the storm hydrograph [9]. Several studies document the effects of increasing the peak stage and the storm duration of the elevated stage on bank storage. Typically, floods rising to higher stages, and lasting for a longer time, allow more stream water to infiltrate into the bank sediments [17,18,21,22]. Chen and Chen [22] examined the effects of increasing peak stage and storm duration on changes in the storage zone. As both peak stage and storm duration increased, the size of the storage zone expanded [22]. Storage zone increases signified water is infiltrating farther into the stream bank sediments, thus delaying the return time and increasing the residence time [18]. Siergieiev et al. [18] further documented the differences of peak stage and storm duration by examining the discharge between the stream and aquifer interface noting that as the peak stage increased, the flux across the boundary increased. While studies have explored how increases in peak stage and storm duration together affect bank storage, an examination as to which factor is more influential has not been performed.

Previous research documenting the effects of increasing peak stage and storm duration on bank storage use both analytical [13,17,23–25] and numerical flow models [10,17,18,22]. Arguing that the transverse (y) dimensional component is only important at the beginning and end of an event, Bates, et al. [26] justifies modeling bank-storage as a two-dimensional process, often the horizontal (x) and vertical (z) dimensions. However, along natural meandering streams, two dimensions might skew the results. As mentioned previously, meandering channels induce parafluvial exchanges across the meander bends [2,3,15,16]. Very few studies use 3-D models [17,22]. Since groundwater and surface water interactions are complex and occur over all dimensions, 3-D modeling is needed to fully understand the bank-storage process [7].

This work modeled bank storage along a meandering stream to investigate how peak stage and storm duration control the volume of bank storage. Peak stage and storm duration were examined separately to ascertain whether one variable influences the volume of bank storage more than the other.

2. Materials and Methods

2.1. Study Site: Little Kickapoo Creek

The model was developed to simulate bank storage along a small reach of Little Kickapoo Creek (LKC), located in central Illinois (Figure 1). The climate of central Illinois is humid continental with cold winters and warm summers; average annual precipitation of the area from 2005 to 2015 was 0.95 m, evenly distributed throughout the year [27]. The site has been previously described (see [3,16,28–33]; presented are the salient information drawn from those works. LKC is a third order, low gradient

(0.002), perennial stream. The stage of LKC can change dramatically in response to high precipitation or snowmelt events. A gauge located south of the study site recorded base-level stage fluctuates between 0.9 to 1.1 m above the streambed; and during high precipitation or snow melting events, the stage can peak up to 4 m depending on the location along the stream. The gauge nearby also showed that the post-storm event stage was asymmetric. After a storm, the stage of LKC typically reaches its maximum stage within a few hours before the stage steadily returns to baseflow (Figure 2). The steady stage drop can take several hours and even up to several days depending on the amount of precipitation.

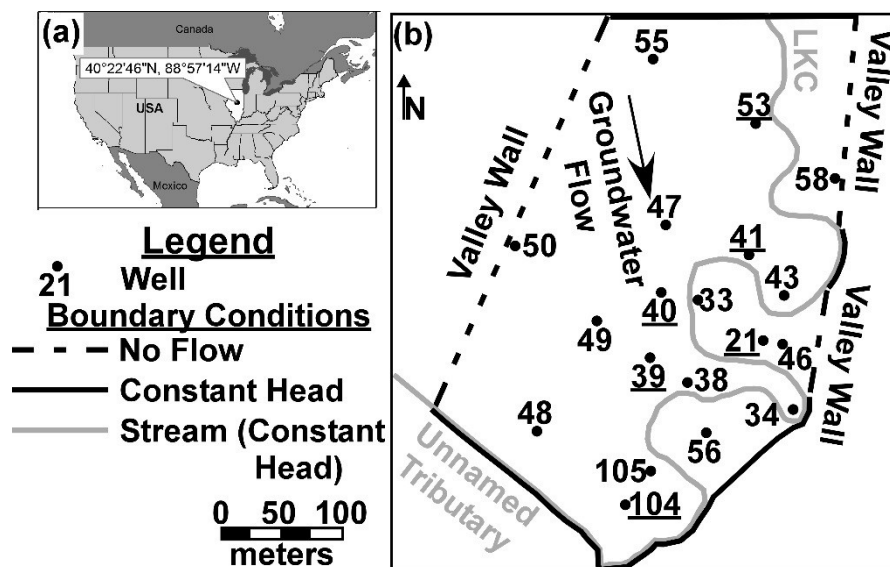


Figure 1. (a) Model area of Little Kickapoo Creek (LKC) in central Illinois, USA (40°22'46" N, 85°57'14" W) (b) Model domain with boundary conditions (black lines), streams (grey), and wells (circles). Groundwater flows to the south-southeast.

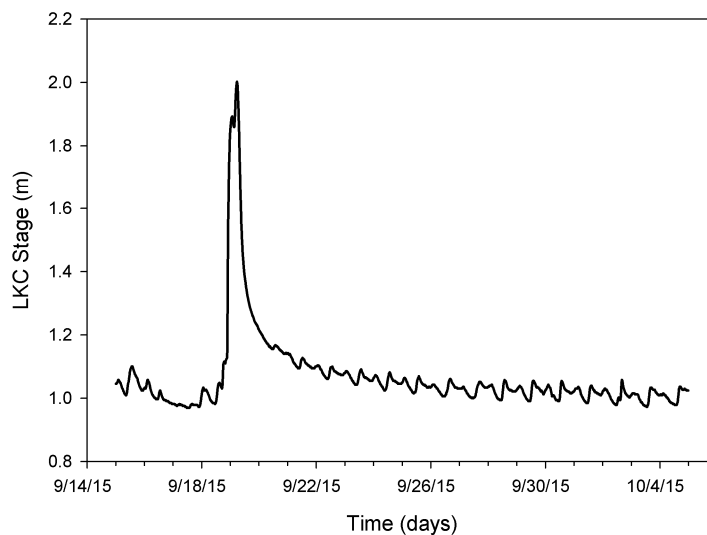


Figure 2. Representative hydrograph of LKC pre-and post-storm event. Stage increases rapidly to a peak of 2 m, which is approximately 1 m of change from baseflow. Other storm events produced similar trends.

LKC is unmodified and meanders through a 300 m wide alluvial valley developed during the Wisconsin glaciation episode. The valley was created by meltwaters that eroded through a low-permeable clay-till, Wedron Formation. Coarse-grained sands and gravels, the Henry Formation, filled the valley. Alluvial deposits, the Cahokia Alluvium, overlie the Henry Formation. Extending

across the valley, the Cahokia Alluvium comprises 2 m of fine-grained sand and clayey silts with organic material. Roots of plants, animal burrows, and worm holes have created macropores in the alluvium resulting in a saturated hydraulic conductivity of 3.5×10^{-6} m/s and an average porosity of 0.25. The Henry Formation, composed of 10 m of poorly-sorted gravels with sands, pinches out at the valley walls. The unit is an unconfined aquifer with a horizontal hydraulic conductivity at 1.0×10^{-4} m/s and specific storage and specific yield values of 0.0007 and 0.021, respectively. The Wedron Group is 70 m of diamicton with a hydraulic conductivity of 1.0×10^{-8} and acts as the lower confining unit.

The base-level of LKC fluctuates 0.2 m but can rise over 4 m following recharge events. The streambed of the LKC is composed of the Henry Formation. Composed of alluvium, the banks of the stream range from sharply incised banks that cut into the alluvium to low-relief depositional point bars. Throughout the aquifer, groundwater flows towards the south-southeast. Changes in stream stage affect the level of water in the wells close to the stream, while wells farther away are controlled more by precipitation.

Bank storage has been documented in the study site, but not explored. Peterson and Sickbert [3], used thermal transport to track hyporheic exchange through a meander neck in the study site. Due to the increased gradient across the meander neck, water flowed through the neck, and the aquifer provided short-term bank storage. Van der Hoven, Fromm and Peterson [32] confirmed the findings with a chloride transport model of the study area. Reported chloride concentrations in LKC range from ~150 to >1000 mg/L, an impact of deicing agents [32,34], while groundwater concentrations have chloride concentrations of ~11.8 mg/L [31,32]. Across the meander neck, groundwater chloride concentrations (~152.4 mg/L) are an order of magnitude higher than groundwater up-gradient from the stream and are similar to the impacted waters of LKC [32].

2.2. Field Data

Groundwater depths were measured at 18 wells across the study site on a bi-weekly basis from 2 February 2016 through 2 August 2016 (Figure 1B). Measured groundwater depths from the wells were compared to steady-state simulations and used to calibrate the numerical model. Pressure transducers located within LKC on the northern and southern edges of the study site recorded water elevation in the stream. These data were used to construct the real-world storm scenarios used in each simulation.

Stream water sampling and discharge measurements occurred on a bi-weekly basis from 2 February 2016 through 28 December 2016. An electromagnetic flow meter was used to measure stream velocity at 0.6 depth, which was incorporated into the velocity-area method to calculate stream discharge. Stream samples were collected in triple-rinsed bottles and filtered before being analyzed for anions (specifically chloride) with a Dionex DX-120 Ion Chromatograph. Two separate sampling events occurred where groundwater samples in six wells were analyzed for chloride on 22 June 2016 and 8 September 2016. Wells included in the sampling were 104, 53, 41, 40, 39, and 21 (Figure 1B). Stream water sampling occurred along the reach towards the southern edge of the study area near well 105. This sampling location is referred to as LKC South.

2.3. Conceptual Model

A conceptual model was constructed based upon the aquifer properties and conditions reported above and were consistent with previous models of the site [28,32,33,35] (Figure 1B). The elevation and extent of the study site were defined using Light Detection and Radar (LiDAR) data in ArcMap [36]. Borehole data were used to delineate the subsurface domain and extent of the glacial outwash. The east/west (x) dimension of the domain was 336 m and the north/south dimension (y) was 429 m. Previous works successfully modeled the system represented by the Cahokia Alluvium and the Henry Formation, the Wedron Formation serving as the lower confining unit [28,32]. The thickness of the Cahokia was 2 m across the entirety of the domain. The thickness of the Henry Formation was variable, maximum 10 m thick under the stream and pinched out at the eastern and western edges. As with the previous models, the Henry Formation and the Cahokia Alluvium were considered homogenous and

isotropic (Cahokia hydraulic conductivity (K) = 3.5×10^{-6} m/s; Henry K = 1.0×10^{-4} m/s). The porosity (n) was 0.25 for the Cahokia and 0.35 for the Henry Formation. Specific storage (S_s) and specific yield (S_y) values for the Henry Formation were 0.0007 and 0.021, and the values for the Cahokia were 0.001 and 0.01, respectively. The boundary conditions along the top of the model were designated as a constant flux, which represented recharge from precipitation. The initial recharge value was set to 10% of the average annual rainfall of 3.01×10^{-10} m/s, based upon a regional model [30]. The bottom boundary is a no flow boundary representing the low permeable Wedron Group [16,28]. The northern, southwestern, and southeastern boundaries were constant head boundaries. The southwestern boundary was set using surveyed elevations of the nearby tributary; while the northern boundary was established using collected observed groundwater elevations [35]. The southeastern boundary had two components with the first being set using observed groundwater elevations in the area and the second was the ending reach of LKC. The elevation of the stream (i.e., stage) represented a constant head boundary at the stream. The eastern and western boundaries were considered no flow boundaries coinciding with the location where the Henry Formation and Cahokia Alluvium pinch out along the valley edge where the Wedron Formation is present.

2.4. Numerical Model

The conceptual model was developed into a numerical model using MODFLOW 2000 [37]. Initial parameters and boundary conditions are presented in Table 1. The Cahokia Alluvium was the top layer (2 m); the Henry Formation had 10 layers (10 m). The contact between the Henry Formation and the confining unit, the Wedron Group, served as the lower no-flow boundary. The cell size of the top layer was $3 \times 3 \times 2$ m and the 10 layers in the Henry Formation were $3 \times 3 \times 1$ m. MODFLOW simulations were conducted under the following assumptions: 3-D, unconfined, heterogeneous, isotropic aquifer. The model was calibrated under steady-state conditions from measured groundwater elevations data collected from the field.

Table 1. Initial and calibrated values employed in the numerical model.

Parameter	Initial Values	Source	Calibrated Values
Henry Formation			
K^1	1.0×10^{-4} m/s	[28]	1.1×10^{-4} m/s
n^2	0.35	[28]	0.35
S_y^3	0.021	[30]	0.021
S_s^4	0.0007	[30]	0.0007
Cahokia Alluvium			
K	3.5×10^{-6} m/s	[28]	6.1×10^{-7} m/s
n	0.25	[28]	0.25
S_y	0.01	Unpublished	0.01
Recharge Rate	3.1×10^{-10} m/s	[27]	3.2×10^{-9} m/s

¹ K – Hydraulic Conductivity; ² n – porosity; ³ S_y – Specific yield; ⁴ S_s – Specific storage

Post-calibration, 36 numerical simulations were conducted under transient-state conditions to investigate the influence of peak stage and storm duration on bank storage. Peak stage was defined as the peak stage of the flood hydrograph, and storm duration was defined as the length of time that the peak stage was sustained throughout each simulation (Figure 3). A gauging station located along LKC south of the study site, showed that most of the storm events over a given year generate a peak stage of ~1 m. Six peak stages, 0.15, 0.3, 0.46, 0.61, 0.76, and 0.91 m, and six storm durations, 1, 3, 5, 7, 9, 10 h, were simulated. Combinations of peak stage and storm duration generated 36 simulations. These hydrographs were constructed based off observed hydrographs for LKC (e.g., Figure 2). For example, if the combination of peak stage of 0.61 m with a storm duration of 5 h was used, the hydrograph would steadily increase towards a peak of 0.61 m at the ninth hour. Then, for

5 h, the peak stage would be sustained until the fourteenth hour, then begin to steadily decrease to pre-peak stage. Each simulation ended at 100 h. However, this study calculated the volume of bank storage (m^3) by using change in storage from the first hour of the simulation across the entirety of the first layer (Cahokia Alluvium). Storage values were calculated and recorded to determine the effects of peak stage and storm duration. Properties of storage values observed were changes in maximum bank storage, flux, amount of storage remaining after 100 h, gradient changes, and storage zone changes.

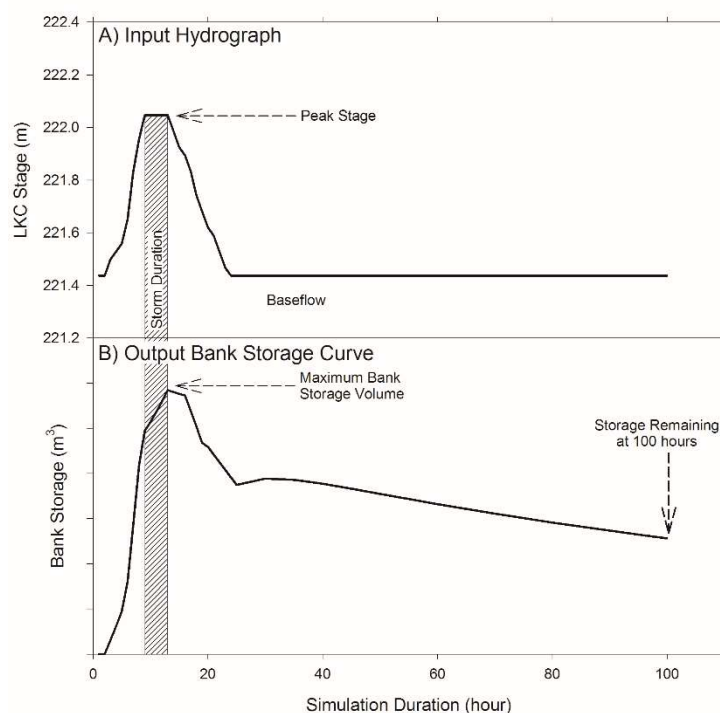


Figure 3. (A) Example of the input hydrograph used in the simulations; peak stage and storm duration are defined. (B) Example of an output bank-storage curve; the variables of maximum bank storage and the storage remaining after 100 h are defined on the curve.

Using IBM SPSS Statistics 24, multiple linear regression models were constructed to predict maximum bank storage (MBS) and storage remaining at 100 h (100). The first model (L_{MBS}) employed peak stage and storm duration as independent variables to predict the dependent variable of maximum bank storage. With the second model (L_{100}), the dependent variable of storage remaining at 100 h was calculated using peak stage and storm duration as independent variables. The analyses generated standardized coefficients by normalizing both independent variables and the dependent variable, which allows for the comparison of independent variables.

3. Results

3.1. Calibration

Manual calibration resulted in modification of the K value for the Cahokia Alluvium and the recharge rate (Table 1). The calibrated K value of the Cahokia Alluvium was 6.1×10^{-7} m/s, an order of magnitude smaller than the initial value, but was consistent with the model developed by Van der Hoven, Fromm and Peterson [32]. The calibrated recharge rate represented 9% of the annual rainfall, which has been used in other models examining the area [28,35]. The calibrated model produced a mean absolute error of 0.15 m and a root mean square error of 0.19 m (Figure 4).

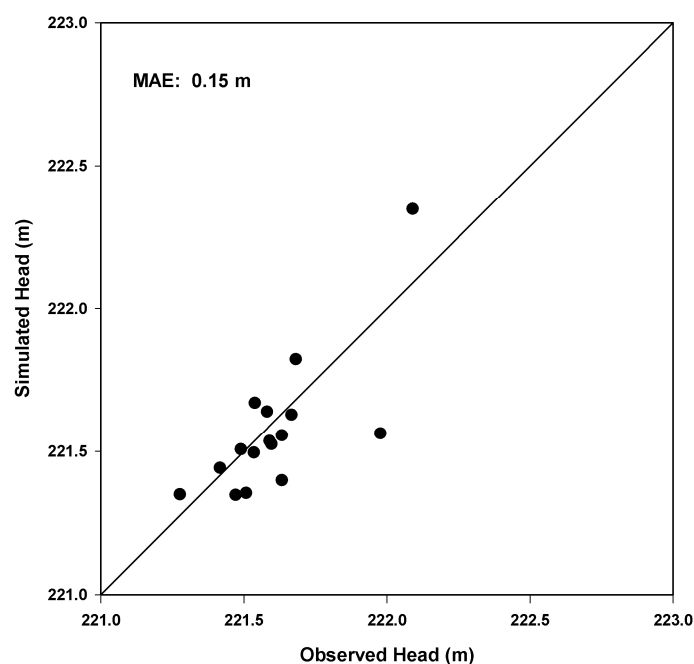


Figure 4. Measured head (groundwater head values observed in the field) versus simulated head (modeled head values at each measuring location). The residuals analysis results in a mean absolute error (MAE) of 0.15 m. Black line shows the 1:1 ratio for an ideal model solution.

The calibrated model indicated a groundwater flow direction of north to south, except for areas within four meters of the stream. Simulated groundwater flow is towards the stream, consistent with previous interpretations that LKC is a gaining stream.

3.2. Bank Storage Simulations

Following model calibration, the 36 model scenarios were simulated for the various combinations of peak stages and storm durations. For each simulation, storage over the entire model was recorded at each hour of the 100 h and subtracted from the first hour to calculate the change in bank storage reported in m^3 . In the interest of preserving space, presented results examine the influence of peak stage and storm duration for only 12 simulations. Six of the simulations examine the variation of peak stage over a constant storm duration of 5 h; the second six simulations focus on a constant peak stage over the various storm durations.

3.3. Peak Stage

In response to the change in stage associated with each simulation, the storage values increase until a maximum bank storage is reached. During this time, water is leaving the stream and entering the adjacent aquifer and is referred to as the fill time. After the maximum storage occurs, water then returns from the aquifer to the stream during what is referred to as the return time. Changes in slope of the fill and return time reflect changes in the discharge of water entering or leaving the aquifer. Increasing peak stage has effects on the discharge of the fill time and return time. Here, increases in peak stage appear to increase both the fill time and return time as the slope of the higher peak stages have steeper slopes (Figure 5). Along LKC, infiltration time for bank storage was much shorter than the return time back to the stream, and even after 100 h, a large portion (33%–64%) of the bank storage had not returned to the stream (Figure 5; Table 2). Overall, the shape of the output bank-storage curve is asymmetrical with a sharp increase until the maximum bank storage is reached, then a sharp decline until the stage of LKC returns to baseflow.

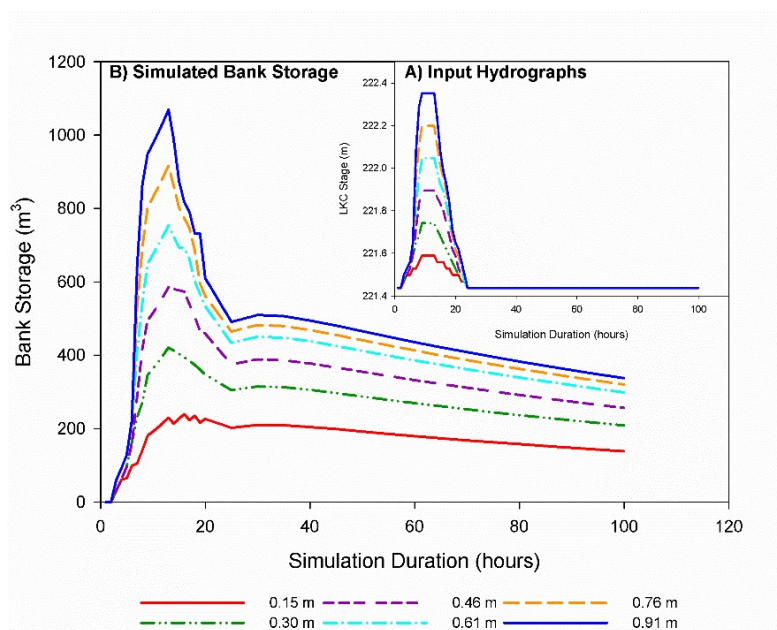


Figure 5. (A) (Inset) Input hydrographs used in numerical simulations. (B) Simulated bank storage for model scenarios with a variable peak stage that reached a maximum value at hour nine and was held constant for 5 h. Storage values are measured as change from beginning of simulation (first hour).

Table 2. Percentage of bank storage remaining at 100 h (% = volume at 100/maximum bank storage).

Storm Duration (h)	Peak Stage (m)					
	0.15	0.3	0.46	0.61	0.76	0.91
1	33%	42%	37%	33%	28%	25%
3	56%	47%	40%	37%	32%	29%
5	61%	50%	44%	40%	35%	32%
7	63%	52%	47%	43%	38%	34%
9	64%	55%	49%	44%	40%	37%
10	64%	55%	52%	45%	41%	38%

Larger peak-stage resulted in greater maximum bank storage volumes and in a greater volume of bank storage remaining after 100 h (Figure 5). Using a constant storm-duration of 5 h coupled with different peak stages (Figure 5A), the effect of increasing stage on bank storage was examined (Figure 5B). For example, the maximum bank storage for a 0.3 m increase was 416.5 m³ with 215.3 m³ remaining in storage after 100 h, while the 0.91 m increase simulation maxed at 1053 m³ with an ending value of 348.3 m³ at 100 h (Figure 5). Increases in peak stage produced a concomitant linear increase in the maximum bank storage for each simulation (Figure 6A). Although higher stage values generated greater banking storage volume remaining after 100 h, the relationship between peak stage and bank storage volume after 100 h was not linear (Figure 6B; Table 2). The percent of storage remaining in the aquifer compared to the maximum bank storage was 61% for the 0.15 m simulation and 33% for the 0.91 m increase.

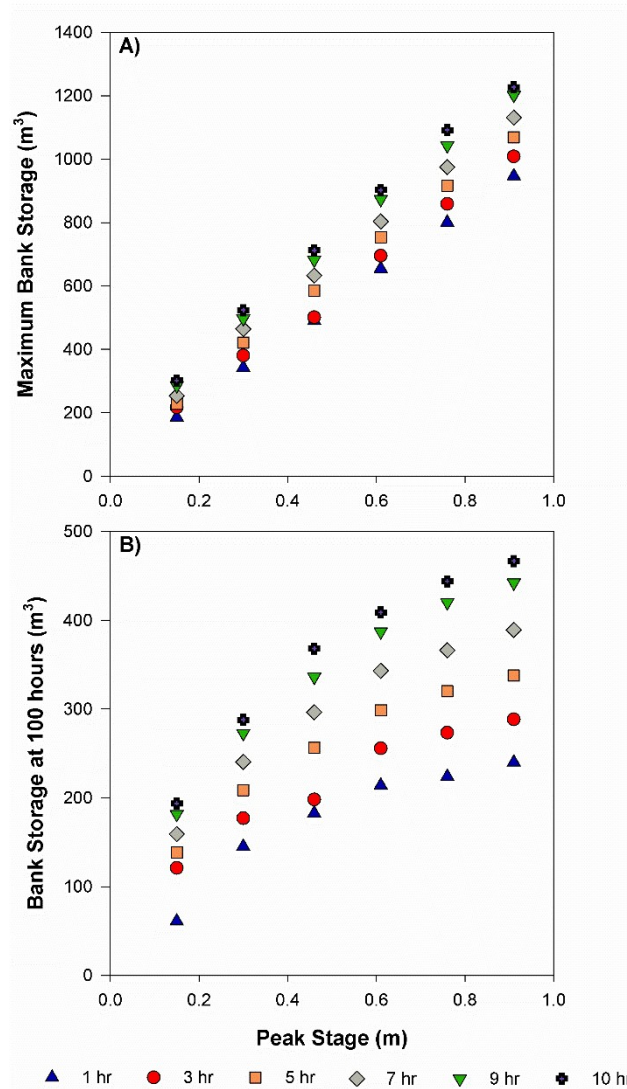


Figure 6. (A) Peak stage versus maximum bank storage and peak stage for all 36 numerical simulations, a positive relationship exists for all storm durations. (B) Relationship between peak stage and bank storage remaining at 100 h for all 36 numerical simulations.

3.4. Storm Duration

Given the similarity among the trials, only six scenarios with a constant stage of 0.61 m and varying storm durations were presented (Figure 7). As storm duration increased, the maximum volume of bank storage increased and the timing of the maximum storage occurred later. For example, the 1 h duration simulation reached peak bank storage of 653.9 m³ 9 h after initiation, while the 10 h duration generated a maximum bank storage of 902.2 m³ at 18 h. Therefore, a 10-fold increase in storm duration increased the maximum bank storage by 1.4. As opposed to increasing peak stage, there were no observed flux differentiations with altering the storm duration due to constant slopes of the fill time and return time as storm duration increased. Longer storms generated greater maximum bank storage, which equated to a higher volume of bank storage remaining after 100 h (Figure 8). For the 1 h duration of a constant 0.61 m stage, bank storage remaining after 100 h was 214 m³, while the 10 h simulation was 408.8 m³. With a 10-fold increase in storm duration, the bank storage remaining increased by 1.9. The percent of storage remaining in the aquifer compared to the maximum bank storage was 33% for the 1 h storm duration and increased to 45% percent for the 10 h duration. For a consistent stage, linear relationships are evident and generate representative and consistent lines among the various stage

values. Longer storm durations generated greater maximum bank storage, following a linear trend for all peak stage values. For all peak stage values, the percentage of bank storage remaining at 100 h increased as storm duration became longer (Table 2). Unlike the influence of stage on volume of bank storage after 100 h (Figure 6B), a linear equation best describes the relationship between storm duration and bank storage at 100 h (Figure 8B).

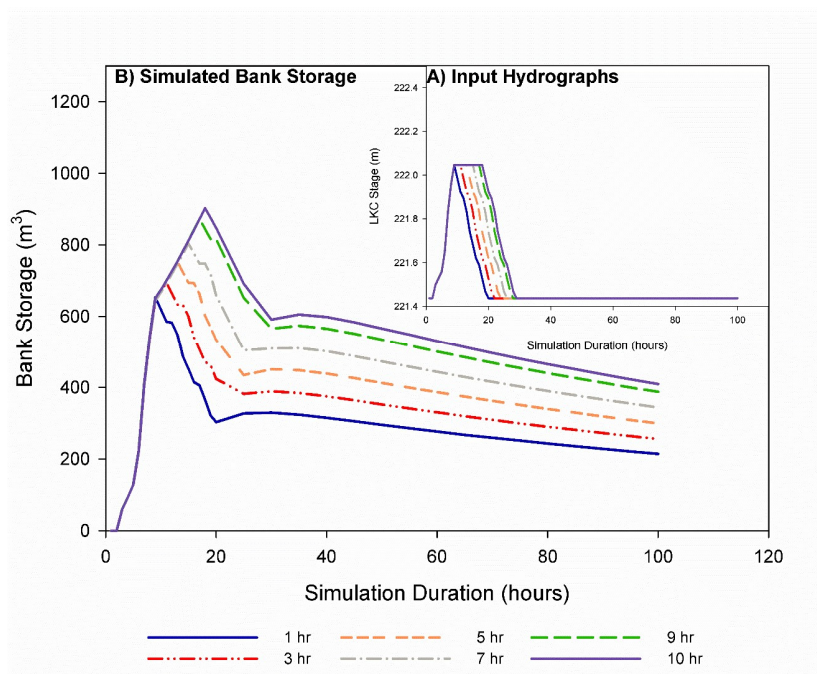


Figure 7. (A) Hydrograph input used in numerical model simulation for the results provided in Figure 6B. (B) Simulation results for model scenarios with a 0.61 m stage peaking at 9 h and held constant for various storm durations. Storage values are measured as change from beginning of simulation (first hour).

The shape of the bank-storage output curve had a similar asymmetrical shape to that of peak stage with a few differences (Figure 7). Like with peak stage, the fill time rose sharply to the maximum value then sharply decreased until the stream returns to baseflow. Once the stream was at baseflow, the remaining storage then steadily returned to the stream over several days. However, the slope of the fill time and return time remained constant, indicating the longer storm duration had limited effect on discharge of the water entering and returning to the stream. While the occurrence of peak storage was consistent when storm duration was constant, the time of occurrence was related to storm duration. Shorter duration storms reached peak bank storage sooner, and longer duration storms experienced peak bank storage later (Figure 8).

3.5. Multiple Linear Regression Analysis

Peak stage and storm duration were strong indicators of maximum bank storage and volumes of bank storage remaining at 100 h. The results L_{MBS} indicate the peak stage and storm duration explained 99.3% of the variance ($r^2 = 0.99$, $F(2,33) = 2450.59$, $p < 0.001$). Both peak stage ($\beta = 0.962$, $p < 0.001$) and storm duration ($\beta = 0.262$, $p < 0.001$) significantly contribute to the calculation of maximum bank storage. With L_{100} , peak stage and storm duration explained 93.6% of the variance ($r^2 = 0.94$, $F(2,33) = 233.73$, $p < 0.001$). The storage remaining at 100 h was correlated to peak stage ($\beta = 0.750$, $p < 0.001$) and storm duration ($\beta = 0.664$, $p < 0.001$). The standardized coefficients indicate that the peak stage is more influential in predicting the maximum bank storage than storm duration. For storage remaining at 100 h, peak stage is more influential than storm duration.

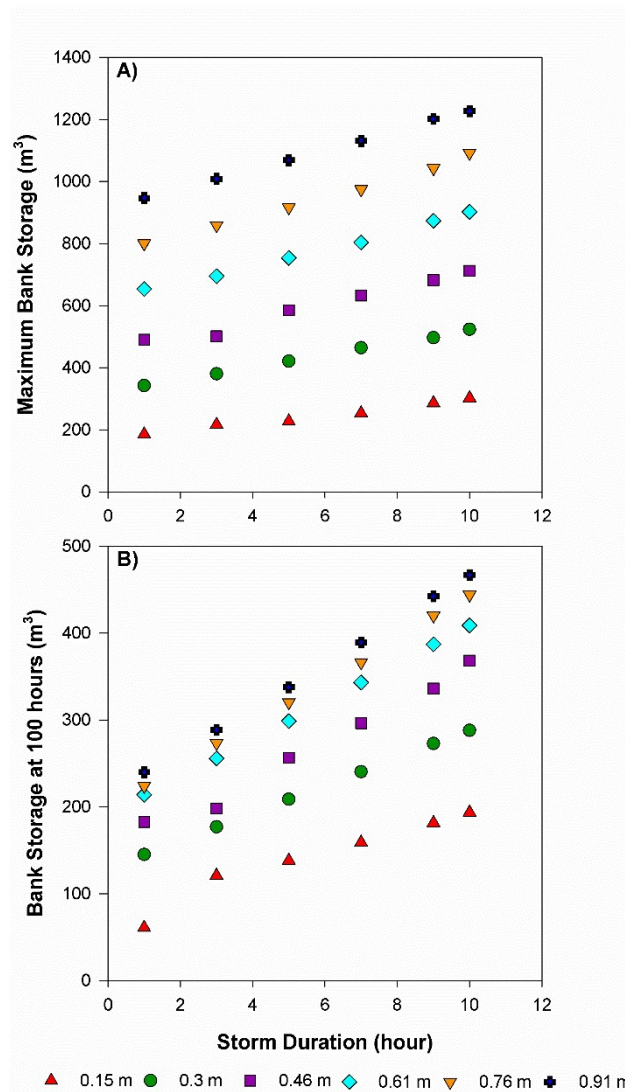


Figure 8. (A) Positive relationship between maximum bank storage and storm duration from all 36 numerical model simulations. (B) Positive relationship between storage remaining at 100 h and storm duration from all 36 numerical model simulations.

4. Discussion

Peak stage and storm duration are both key factors in controlling the bank-storage process. Previous research examined both peak stage and storm duration together, documenting increases in both parameters increased the amount of storage that occurred [17,18,21,22]. The purpose of the project was to identify which factor influences the amount of bank storage more. The linear regression analysis indicated that peak-stage is ~3.6 times more correlated than storm duration in determining the maximum bank-storage volume that occurs after a storm event. When determining the storage remaining at 100 h, peak stage is still more influential in determining that value. The results showed peak stage and storm duration affect different areas of the bank-storage process, and as such, neither factor, storm duration or peak stage, was more important than the other.

4.1. Peak Stage Influences

Peak stage was more influential than storm duration in determining the maximum bank storage that occurs over a given storm event. Increases in peak stage led to greater change in the maximum bank storage volumes than increasing storm duration (Figures 6 and 8). The increases in maximum bank

storage due to increasing peak stage documented here are consistent with previous work [17,18,21]. Employing a 1-D analytical model, [17] simulated peak stages of 1, 2, and 3 m that generated maximum bank storage values of 30, 60, and 90 m³/m, respectfully. Thus, a three-fold increase in peak stage resulted in a three-fold increase in maximum bank storage. In the current 3-D simulations, a three-fold increase in peak stage resulted in a 2.5-fold increase in maximum bank storage.

As peak stage increases, the maximum bank storage increases as well, but the time of each maximum amount occurs at the same time (Figure 5). This suggests that increasing the peak stage increases the discharge of water in and out of the aquifer. The increases in discharge entering and leaving the banks are a result from the observed increase in hydraulic gradient near the stream. As expected, increasing peak stage allows a large volume of water to enter the bank sediments at a faster rate as compared to lower peak stages. Since high peak stage storm events allow higher maximum bank-storage volumes to occur but less actual retention of that storage, these high peak stage storm events can act as flushing events. These events have the potential to flush previous bank storage.

While peak stage was more influential in determining the volume of storage that occurred, it had less effect than storm duration on retention of storage. This is indicated by two observations: (1) Increases in peak stage decreased the percentage of storage remaining in the aquifer at 100 h (Table 2); and (2) at high peak stages the increases of storage zone volume were minimized. The physical properties (hydraulic conductivity, porosity, and permeability) of the Cahokia Alluvium limit deep infiltration of stream water into the bank sediments, which allows the water to return to the stream faster after a stage decrease. This limitation explains the asymmetrical shape of the bank-storage output curve associated with increasing peak stage. Increases in maximum bank storage due to increasing peak stage occur due to the exposure of more bank sediment material. However, a large proportion of that bank storage returned quickly because the water did not infiltrate deep into the sediment at higher peak stages.

4.2. Storm Duration Influences

Although peak stage was more influential than storm duration when determining the storage volume remaining at 100 h, storm duration appears to be more efficient at the retention of bank storage than peak stage. Three observations contributed to the relationship. First, the percent of bank storage remaining at 100 h increased with storm duration and decreased with peak stage (Table 2). Second, storage remaining at 100 h appeared to increase continuously for storm duration (Figure 8B) and leveled off for peak stage (Figure 6B). Finally, increasing storm duration led to greater storage zone size while higher peak stages provided little change in storage zone size.

Maximum bank storage increased slightly with increasing storm duration. With a constant peak stage, the additional bank storage occurred through expanding the storage zone laterally. Soil properties of the bank sediments played a role in dictating the amount of bank storage that can infiltrate into the bank sediments. Therefore, increasing the peak stage allows for a larger maximum volume to occur, the water did not infiltrate deep enough to be retained for long periods. Increasing the storm duration; however, minimized the effects of the soil properties, and water penetrated deeper into the bank sediments, generating a larger back storage volume. Chen et al. [22] reported increases in storage zone volume delayed the return time of water to the stream as bank storage waters were retained. The 3-D simulations showed increases in storm duration caused an increase in maximum bank-storage volume and storage zone size, consistent with other reported models [18,21,22].

4.3. Implications along LKC

Bank storage studies have used 1-D, 2-D, and 3-D models to evaluate how variables control the bank storage process; however, three dimensions are needed to accurately quantify volume of bank storage that occurs over each simulation. Bank storage is defined as the change in volume of storage per unit of the stream (m³/m); however, the results above were reported as change in volume across the entirety of the first layer in the model (m³). The length of LKC during each simulation

was 1152 m, thus the range of maximum bank storage values were from 0.185 to 1.05 m³/m. During most of the 36 simulations, less than 1.0 m³/m occurred along the stream. However, the simulations illustrated that most of the bank storage occurred across the meander bends and less infiltrated along the straight reaches of the stream. For example, the hydraulic gradient change due to the increase in peak stage was observed within 4 m of LKC. However, as the peak stage and storm duration increase, the volume of the bank storage zone swelled across the meander bends, with little to no change along the straight reaches of the stream. The shape of the output bank-storage curve also indicated this response, especially for the higher peak stage simulations. At high peak stages, the bank storage increased quickly to the maximum volume and then decreased quickly until LKC returned to baseflow (Figure 5). The remaining storage slowly returned to the stream over several days.

The lack of infiltration along the straight reaches and the limited depth of infiltration into the bank sediments led to a large portion of the bank storage quickly returning to the stream. Water infiltrating across the meander bend penetrated farther and had a longer return time. The shallow slope return time beginning as soon as LKC returned to baseflow can be attributed to storage across the meander bends. With longer flow paths across the meander bends, bank-storage water took days to return to the stream. The meander lobe increases the cross-sectional area over which water would infiltrate, which has been shown to increase storage volume and retention time [20].

The influence of the meander bend would not have been captured if the model simulated one or two dimensions. There are two consequences of using a two-dimensional model along a meander stream. If a two-dimensional model were created along a straight reach and the bank-storage values were extrapolated along the river, the values would be underestimated. Likewise, if a two-dimensional model were created along the meander bend, the values would be overestimated. Ha, Koh, Yum and Lee [17] noted a similar finding when comparing 1-D and 3-D models. For a 1-D model of a river reach, the maximum bank-storage values were above 10 m³/m, compared to 0.05 m³/m for the same stretch simulated in 3-D.

Along LKC and within the watershed, non-point-source pollution of road salts has been reported [30,34,38]. As with those and other reported studies [32,39–41], measured chloride concentrations in LKC waters varied seasonally, with the highest concentrations in the winter and lowest concentrations in the fall. The minimum chloride concentration, 38 mg/L, was elevated compared to the documented background concentration of ~15 mg/L in central Illinois [42]. Researchers have attributed non-winter, elevated chloride concentrations to large masses of chloride moving through the groundwater that originated in areas with high urban land use [39,41,43]. However, Ludwikowski and Peterson [30] did not observe plumes of chloride movement to streams in their simulation of chloride transport in the LKC watershed. Our simulation results indicated that the elevated concentrations of chloride may be a result of stored chlorides released from storage along the bank sediments and across meander bends of LKC. Peterson and Sickbert [3] calculated travel times of up to 200 days across the meander. Similarly, Van der Hoven, Fromm and Peterson [32] showed, through simulation, that chloride transport through the meander bend required 60 to 200 days. During the winter months, when chloride concentrations were the highest and stream stages tend to be elevated, stream water migrated into the meander bends and was temporarily stored. Throughout summer, several high peak stage events produced bank storage that flushed the high chloride waters within the meander into the stream. This interpretation is consistent with the above results, as the several high peak stage and low storm duration events occur in the summer.

5. Conclusions

Neither peak stage nor storm duration were more important than the other, in terms of effecting the bank-storage process. Other research documents similar effects due to increasing peak stage and storm duration. However, this study, using a 3-D numerical model, documented peak stage being statistically more influential in determining the maximum bank storage, ~3.6 times, and the bank storage occurring at 100 h, ~1.1×. While it was more influential at determining the storage remaining

at 100 h, storm duration influenced the retention of bank storage by allowing stream water to infiltrate farther into the bank sediments. In addition, as peak stage increased, the storage remaining at 100 h begins to level off suggesting that, even at the highest stages, water could only infiltrate so far before the gradient reverse, returning the water to the stream. Meandering bends along a stream induced bank storage. Output bank-storage curves, distribution of chloride concentrations across the study site, and storage zone changes along LKC show that most of the stream–aquifer interactions occurred along the meander bends.

Author Contributions: Conceptualization, L.P.C. and E.W.P.; methodology, L.P.C. and E.W.P.; software, L.P.C.; validation, L.P.C. and E.W.P.; formal analysis, L.P.C. and E.W.P.; investigation, L.P.C. and E.W.P.; resources, L.P.C. and E.W.P.; data curation, E.W.P.; writing—original draft preparation, L.P.C. and E.W.P.; writing—review and editing, E.W.P. and L.P.C.; visualization, L.P.C. and E.W.P.; supervision, E.W.P.; project administration, E.W.P.; funding acquisition, E.W.P.”

Funding: This research was funded by the Illinois Water Resource Center, grant number A16-0097-001.

Acknowledgments: The authors thank the Bloomington-Normal Wastewater District for access to the study location.

Conflicts of Interest: The authors declare no conflicts of interest. The funders had no role in the design of the study; in the collection, analyses, or interpretation of data; in the writing of the manuscript, or in the decision to publish the results.

References

1. Winter, T.C. *Ground Water and Surface Water: A Single Resource*; U.S. Geological Survey: Reston, VA, USA, 1998.
2. Boano, F.; Camporeale, C.; Revelli, R.; Ridolfi, L. Sinuosity-driven hyporheic exchange in meandering rivers. *Geophys. Res. Lett.* **2006**, *33*. [[CrossRef](#)]
3. Peterson, E.W.; Sickbert, T.B. Stream water bypass through a meander neck, laterally extending the hyporheic zone. *Hydrogeol. J.* **2006**, *14*, 1443–1451. [[CrossRef](#)]
4. Cranswick, R.H.; Cook, P.G. Scales and magnitude of hyporheic, river-aquifer and bank storage exchange fluxes. *Hydrol. Process.* **2015**, *29*, 3084–3097. [[CrossRef](#)]
5. Wroblicky, G.J.; Campana, M.E.; Valett, H.M.; Dahm, C.N. Seasonal variation in surface-subsurface water exchange and lateral hyporheic area of two stream-aquifer systems. *Water Resour. Res.* **1998**, *34*, 317–328. [[CrossRef](#)]
6. Woessner, W.W. Stream and fluvial plain ground water interactions: Rescaling hydrogeologic thought. *Ground Water* **2000**, *38*, 423–429. [[CrossRef](#)]
7. Sophocleous, M. Interactions between groundwater and surface water: The state of the science. *Hydrogeol. J.* **2002**, *10*, 52–67. [[CrossRef](#)]
8. Boulton, A.J.; Findlay, S.; Marmonier, P. The functional significance of the hyporheic zone in streams and rivers (review). *Annu. Rev. Ecol. Syst.* **1998**, *29*, 59–81. [[CrossRef](#)]
9. Brunke, M.; Gonser, T. The ecological significance of exchange processes between rivers and groundwater. *Freshw. Biol.* **1997**, *37*, 1–33. [[CrossRef](#)]
10. Squillace, P.J. Observed and simulated movement of bank-storage water. *Ground Water* **1996**, *34*, 121–134. [[CrossRef](#)]
11. Kondolf, G.M.; Maloney, L.M.; Williams, J.G. Effects of bank storage and well pumping on base-flow, carmel-river, monterey-county, california. *J. Hydrol.* **1987**, *91*, 351–369. [[CrossRef](#)]
12. Menció, A.; Galán, M.; Boix, D.; Mas-Pla, J. Analysis of stream–aquifer relationships: A comparison between mass balance and darcy’s law approaches. *J. Hydrol.* **2014**, *517*, 157–172. [[CrossRef](#)]
13. Cooper, H.H.; Rorabaugh, M.I. *Ground-Water Movements and Bank Storage due to Flood Stages in Surface Streams*; Water Supply Paper 1536 J; U.S. Government Printing Office: Washington, DC, USA, 1963.
14. Squillace, P.J.; Thurman, E.M.; Furlong, E.T. Groundwater as a nonpoint source of atrazine and deethylatrazine in a river during base flow conditions. *Water Resour. Res.* **1993**, *29*, 1719–1729. [[CrossRef](#)]
15. Cardenas, M.B.; Wilson, J.L.; Zlotnik, V.A. Impact of heterogeneity, bed forms, and stream curvature on subchannel hyporheic exchange. *Water Resour. Res.* **2004**, *40*. [[CrossRef](#)]

16. Peterson, E.W.; Benning, C. Factors influencing nitrate within a low-gradient agricultural stream. *Environ. Earth Sci.* **2013**, *68*, 1233–1245. [[CrossRef](#)]
17. Ha, K.; Koh, D.C.; Yum, B.W.; Lee, K.K. Estimation of river stage effect on groundwater level, discharge, and bank storage and its field application. *Geosci. J.* **2008**, *12*, 191–204. [[CrossRef](#)]
18. Siergieiev, D.; Ehlert, L.; Reimann, T.; Lundberg, A.; Liedl, R. Modelling hyporheic processes for regulated rivers under transient hydrological and hydrogeological conditions. *Hydrol. Earth Syst. Sci.* **2015**, *19*, 329–340. [[CrossRef](#)]
19. Sjodin, A.; Lewis, W.M.; Saunders, J.F. Analysis of groundwater exchange for a large plains river in Colorado (USA). *Hydrol. Process.* **2001**, *15*, 609–620. [[CrossRef](#)]
20. Doble, R.; Brunner, P.; McCallum, J.; Cook, P.G. An analysis of river bank slope and unsaturated flow effects on bank storage. *Ground Water* **2012**, *50*, 77–86. [[CrossRef](#)]
21. Todd, D.K. Ground-water flow in relation to a flooding stream. *Proc. Am. Soc. Civ. Eng.* **1955**, *81*, 1–20.
22. Chen, X.; Chen, X. Stream water infiltration, bank storage, and storage zone changes due to stream-stage fluctuations. *J. Hydrol.* **2003**, *280*, 246–264. [[CrossRef](#)]
23. Barlow, P.M.; DeSimone, L.A.; Moench, A.F. Aquifer response to stream-stage and recharge variations. II. Convolution method and applications. *J. Hydrol.* **2000**, *230*, 211–229. [[CrossRef](#)]
24. Gill, M.A. Bank storage characteristics of a finite aquifer due to sudden rise and fall of river level. *J. Hydrol.* **1985**, *76*, 133–142. [[CrossRef](#)]
25. Hunt, B. Bank-storage problem and the Dupuit approximation. *J. Hydrol. Eng.* **2005**, *10*, 118–124. [[CrossRef](#)]
26. Bates, P.D.; Stewart, M.D.; Desitter, A.; Anderson, M.G.; Renaud, J.P.; Smith, J.A. Numerical simulation of floodplain hydrology. *Water Resour. Res.* **2000**, *36*, 2517–2529. [[CrossRef](#)]
27. Illinois State Geological Survey. *Illinois State Climatologist Data*; Illinois State Water Survey: Champaign, IL, USA, 2016; Available online: <http://www.isws.illinois.edu/data/climatedb/data.asp> (accessed on 6 February 2017).
28. Ackerman, J.R.; Peterson, E.W.; Van der Hoven, S.; Perry, W. Quantifying nutrient removal from groundwater seepage out of constructed wetlands receiving treated wastewater effluent. *Environ. Earth Sci.* **2015**, *74*, 1633–1645. [[CrossRef](#)]
29. Bastola, H.; Peterson, E.W. Heat tracing to examine seasonal groundwater flow beneath a low-gradient stream. *Hydrogeol. J.* **2016**, *24*, 181–194. [[CrossRef](#)]
30. Ludwikowski, J.J.; Peterson, E.W. Transport and fate of chloride from road salt within a mixed urban and agricultural watershed in Illinois (USA): Assessing the influence of chloride application rates. *Hydrogeol. J.* **2018**, *26*, 1123–1135. [[CrossRef](#)]
31. Peterson, E.W.; Hayden, K.M. Transport and fate of nitrate in the streambed of a low-gradient stream. *Hydrol.* **2018**, *5*, 55. [[CrossRef](#)]
32. Van der Hoven, S.J.; Fromm, N.J.; Peterson, E.W. Quantifying nitrogen cycling beneath a meander of a low gradient, n-impacted, agricultural stream using tracers and numerical modelling. *Hydrol. Process.* **2008**, *22*, 1206–1215. [[CrossRef](#)]
33. Ludwikowski, J.; Malone, D.H.; Peterson, E.W. *Surficial Geologic Map, Bloomington East Quadrangle, Mclean County, Illinois*; Illinois State Geological Survey, Ed.; Illinois State Geological Survey: Champaign, IL, USA, 2016; Available online: <http://isgs.illinois.edu/maps/isgs-quads/surficial-geology/student-map/bloomington-east> (accessed on 9 January 2017).
34. Lax, S.M.; Peterson, E.W.; Van der Hoven, S. Quantifying stream chloride concentrations as a function of land-use. *Environ. Earth Sci.* **2017**, *76*, 12. [[CrossRef](#)]
35. Basu, A. *Quantifying n Cycling between Groundwater and Surface Water Using Numerical Modeling and Mass Flux Calculations*; Illinois State University: Normal, IL, USA, 2007.
36. Illinois State Geological Survey. *Illinois Geospatial Data Clearinghouse, Lidar Data Set, Mclean County*; Illinois State Geological Survey: Champaign, IL, USA, 2014; Available online: <https://clearinghouse.isgs.illinois.edu/data/elevation/illinois-height-modernization-ilhmp-lidar-data> (accessed on 9 January 2017).
37. Harbaugh, A.W.; Banta, E.R.; Hill, M.C.; McDonald, M.G. *Modflow-2000, the U.S. Geological Survey Modular Ground-Water Model-User Guide to Modularization Concepts and the Ground-Water Flow Process*; Open-File Report 00-92; U.S. Geological Survey: Reston, VA, USA, 2000; p. 134.
38. Lax, S.; Peterson, E.W. Characterization of chloride transport in the unsaturated zone near salted road. *Environ. Geol.* **2009**, *58*, 1041–1049. [[CrossRef](#)]

39. Kelly, W.R. Long-term trends in chloride concentrations in shallow aquifers near Chicago. *Ground Water* **2008**, *46*, 772–781. [[CrossRef](#)]
40. Meriano, M.; Eyles, N.; Howard, K.W.F. Hydrogeological impacts of road salt from Canada's busiest highway on a Lake Ontario watershed (Frenchman's Bay) and lagoon, City of Pickering. *J. Contam. Hydrol.* **2009**, *107*, 66–81. [[CrossRef](#)]
41. Corsi, S.R.; De Cicco, L.A.; Lutz, M.A.; Hirsch, R.M. River chloride trends in snow-affected urban watersheds: Increasing concentrations outpace urban growth rate and are common among all seasons. *Sci. Total Environ.* **2015**, *508*, 488–497. [[CrossRef](#)]
42. Panno, S.V.; Hackley, K.C.; Hwang, H.H.; Greenberg, S.E.; Krapac, I.G.; Landsberger, S.; O'Kelly, D.J. Characterization and identification of Na-Cl sources in ground water. *Ground Water* **2006**, *44*, 176–187. [[CrossRef](#)]
43. Bester, M.L.; Frind, E.O.; Molson, J.W.; Rudolph, D.L. Numerical investigation of road salt impact on an urban wellfield. *Ground Water* **2006**, *44*, 165–175. [[CrossRef](#)]



© 2019 by the authors. Licensee MDPI, Basel, Switzerland. This article is an open access article distributed under the terms and conditions of the Creative Commons Attribution (CC BY) license (<http://creativecommons.org/licenses/by/4.0/>).